

Particle acceleration and sources in the November 1997 solar energetic particle events

G. M. Mason,^{1,2} C. M. S. Cohen,³ A. C. Cummings,³ J. R. Dwyer,¹ R. E. Gold,⁴ S. M. Krimigis,⁴ R. A. Leske,³ J. E. Mazur,⁵ R. A. Mewaldt,³ E. Möbius,⁶ M. Popecki,⁶ E. C. Stone,³ T. T. von Rosenvinge,⁷ and M. E. Wiedenbeck⁸

Abstract. We report studies of two large solar energetic particle (SEP) events on Nov. 4 and 6, 1997 that were observed using advanced energetic particle detectors on the ACE and the Wind spacecraft. Both events showed enriched Fe/O, and had a ~ 1 MeV/n $^3\text{He}/^4\text{He}$ ratio $= 2.1 \times 10^{-3}$, 4 times the coronal value. The Nov. 6 event had exceptionally hard spectra, with much higher intensities of high energy (10s of MeV) particles than the Nov. 4 event, yet below 1 MeV/n the intensities in the Nov. 6 event were lower than for Nov. 4. Strong, complex temporal variations observed for ~ 120 keV Fe/O contrasted with only gradual changes of this ratio at ~ 25 MeV/n. A spectral break was observed in the Nov. 6 event, wherein below a few MeV/n the spectra became harder. Taken together, these observations point to different seed and acceleration mechanisms dominating at low and high energies in these events.

Introduction

High energy particle acceleration at the Sun is associated with the most energetic astrophysical phenomenon occurring in the solar system: the explosive release of magnetic energy in the corona. By observing the ions accelerated in SEP events, we can obtain information about the physical mechanisms causing the acceleration, the source site conditions, and the mechanisms of transport of the particles to the observer in interplanetary space. Energetic particles accelerated in large events were understandably believed to have their origin at the site of the optical flare itself [Reinhard and Wibberenz, 1974] and gamma-ray and neutron observations clearly demonstrate that in some events particles are accelerated essentially simultaneously with the photon signatures at the flare site [Ramaty and Murphy, 1987]. However, for the particle populations observed in interplanetary space, a lack of evidence for propagation of the particles over large distances in the solar atmosphere, along with a growing appreciation of the importance of shock acceleration and its relation to coronal mass ejections (CMEs) led to the current view that for large interplanetary events large scale shocks associated with the events lead to substantial acceleration of particles at significant distances from the Sun (10s of solar radii or more) [Mason et al., 1984; Cane et al., 1988].

Observations

The energetic particle observations reported here were carried out with the Ultra Low Energy Isotope Spectrometer (ULEIS), the Solar Energetic Particle Ionic Charge Analyzer (SEPICA), and the Solar Isotope Spectrometer (SIS) on the ACE spacecraft, and the EPACT/STEP sensor on the Wind spacecraft [Mason et al., 1998; Möbius et al., 1998a; Stone et al., 1998; von Rosenvinge et al., 1995]. During the Nov. 4-11, 1997 period both spacecraft were well upstream of the Earth's magnetosphere ($> 100 R_E$). Figure 1 shows oxygen (O) intensities from ACE with markers for other events during this interval. The first event was an X2/2B flare at S14W34° in active region 8100 beginning at 05:54 UT on Nov. 4, 1997 (day 308 – from *Solar Geophysical Data, Part II*). The SOHO spacecraft observed a CME from this event, and the associated shock was observed by the ACE magnetic field and solar wind instruments at approximately 22:00 on Nov. 6 (day 310) followed by a magnetic cloud (Nov. 7 05:00 – Nov. 8 12:00) detected on Wind. A second flare erupted at S18W63° from the same active region at 11:22 on Nov. 6; this event was an X9/2B event that produced ground level increases in neutron monitors (K. R. Pyle, *private communication*), strong gamma-ray emission of C, O, Ne, Mg, Si and Fe and neutron capture lines (M. Yoshimori, *private communication*), and a CME whose associated shock was detected by ACE at $\sim 10:00$ on Nov. 9 (day 313). Both events produced Type II radio bursts. Note from the Figure that the passage of the first shock, with the associated peak in low energy intensities, nearly coincided with the rise-phase of the Nov. 6 particle event. The first shock produced large intensity enhancements for low energy O, with easily observable distortions of the time-intensity profiles up to ~ 2 MeV/n; at higher energies this shock passage did not produce large intensity increases, although such increases could have been masked in part by the rise phase of the day 310 event. The second (“weak”) shock passage, on day 313, is associated with a slight increase in particle intensities below ~ 500 keV/n.

Solar wind speeds during this period varied between ~ 300 – 460 km/s; extrapolating these speeds back to the Sun yields connection longitudes between 50 and 77° . For the Nov. 4 event the distance from the event site to the nominal connection point was about 40° at the onset, decreasing to a few degrees after three days. For the Nov. 6 event, the nominal magnetic connection site was $\sim 15^\circ$ from the flare at the onset, increasing to $\sim 40^\circ$ after three days. Thus, both events were reasonably “well connected”, with the prompt rises of high energy intensities seen in Figure 1. A major feature of the intensities is that the Nov. 6 SEP event produces intensities smaller than the Nov. 4 event at low energies, while at high energies the opposite is true.

The time-intensity profiles in Figure 1 deviate from idealized smooth trends – while some of these features are due to statistical fluctuations, others are significant. This is explored further in Figure 2, which shows low and high energy O intensities in the upper panel, and the ratio of Fe/O in the lower panels, with the shock passage on day 310 marked by yellow shading. At 120 keV/n the following features are seen in the Fe/O ratio: (1) an initial smooth decrease in the first SEP event,

¹ Department of Physics, University of Maryland, College Park, MD (e-mail: mason@sampx3.umd.edu)

² Institute for Physical Science and Technology, University of Maryland

³ California Institute of Technology, Pasadena, CA

⁴ Johns Hopkins University / Applied Physics Laboratory, Laurel, MD

⁵ The Aerospace Corporation, Los Angeles, CA

⁶ University of New Hampshire, Durham, NH

⁷ NASA / Goddard Space Flight Center, Greenbelt, MD

⁸ Jet Propulsion Laboratory, Pasadena, CA

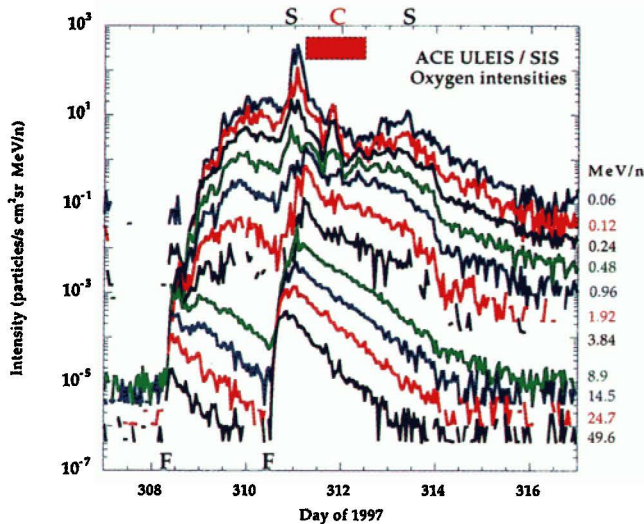


Figure 1. 1-hr average oxygen intensities from 60 keV/n to 50 MeV/n from ACE during the Nov. 1997 events; flare times are marked F; shock passages at ACE are marked S; the red box marked C shows the time of a magnetic cloud passage.

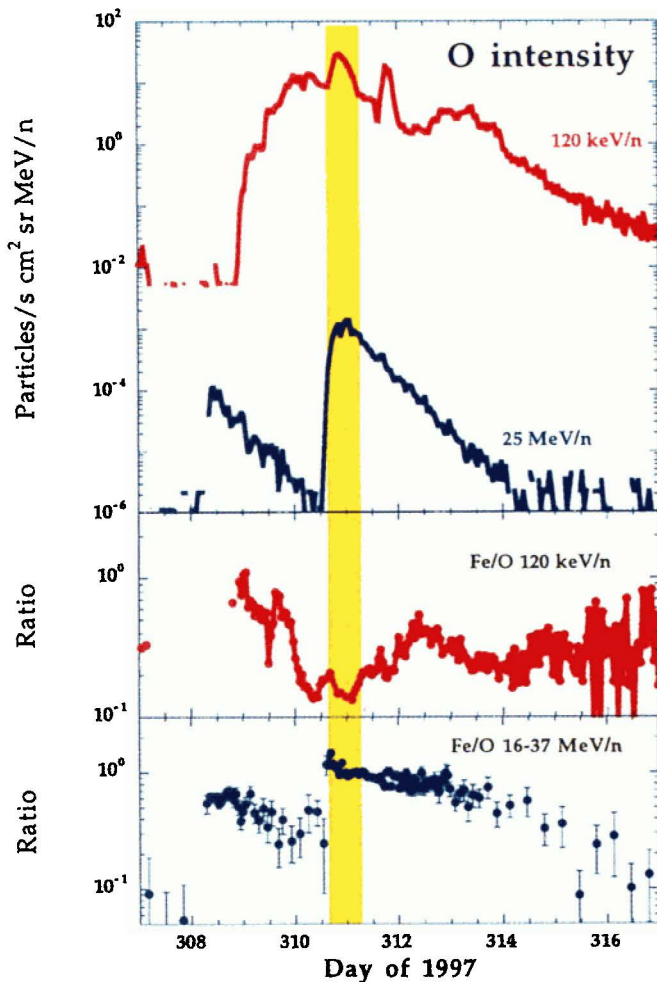


Figure 2. Upper panel: O intensities from ACE/SIS and Wind/EPACT at high and low energies. Yellow shaded area marks first shock passage. Lower panels: Fe/O ratio at 120 keV/n and 16-37 MeV/n.

similar to that seen at the higher energy, followed by (2) a large (factor of 5) drop at about day 310.0, (3) little change during first shock passage, followed by (4) an increase around day 312.5 in coincidence with the arrival of particles from the second event. The striking (factor of ~ 5) decrease in 120 keV/n Fe/O near day 310.0 is caused by a drop in the Fe intensity while the O intensity continues to increase. After day 314, fluctuations are statistical. In contrast, the 16-37 MeV/n Fe/O ratio shows simpler variations, decreasing by a factor of ~ 2 over the course of each event.

Figure 3 shows the average composition for major elements for the Nov. 6 event (results for the Nov. 4 event are similar). The ACE measurements are normalized to O and are compared to SEP average abundances in the energy range 5-12 MeV/n from Reames [1995]. For elements between C and S ($Z=6$ to 16), the abundances are similar over a very broad energy range from 150 keV/n to ~ 60 MeV/n. Compared to the average SEP value, Fe/O is enhanced by a factor of 3-4 at the lower energies, and by a factor of 8 for 12-60 MeV/n. Such ranges of Fe/O variation have been observed previously [Cook *et al.*, 1984; Mazur *et al.*, 1993; Reames, 1995]. Mazur *et al.* [1993] have shown that the event to event variations are generally smaller at low energies, as seen here. Figure 4 shows the 0.5-2.0 MeV/n $^3\text{He}/^4\text{He}$ ratio for the Nov. 6 event. The observed ratio of $(2.1 \pm 0.08) \times 10^{-3}$ is the lowest finite value of this ratio ever reported; nevertheless it is a factor of 4 above the average solar wind value [Ogilvie *et al.*, 1980], and is below limits (usually $\sim 10\%$) often used to identify ^3He -rich events. The $^3\text{He}/^4\text{He}$ ratio in the Nov. 4 event is similar. The arrival time of mass < 3.5 AMU events shown in Figure 4 was uniform in time, with 20 events detected on day 312 and 16 events on day 313. ^3He enhancements have been reported in two large SEP and gamma-ray events [Van Hollebeke *et al.*, 1990] that also showed large Fe/O abundances; however, the $^3\text{He}/^4\text{He}$ enrichment in those events was ~ 50 -170 times coronal values, ~ 10 to 40 times larger than in the Nov. 1997 events.

Over the broad range of energies presented here, velocity dispersion causes significant differences in the duration of the event, increasing from 1-2 days at higher energies to the order of a week at low energies (see Figure 1). Under these circumstances, event-averaged particle intensities may be somewhat misleading since time periods of length suitable for the low energy particles contain significant intervals where the high energy particles have decayed away. To explore spectral forms, we

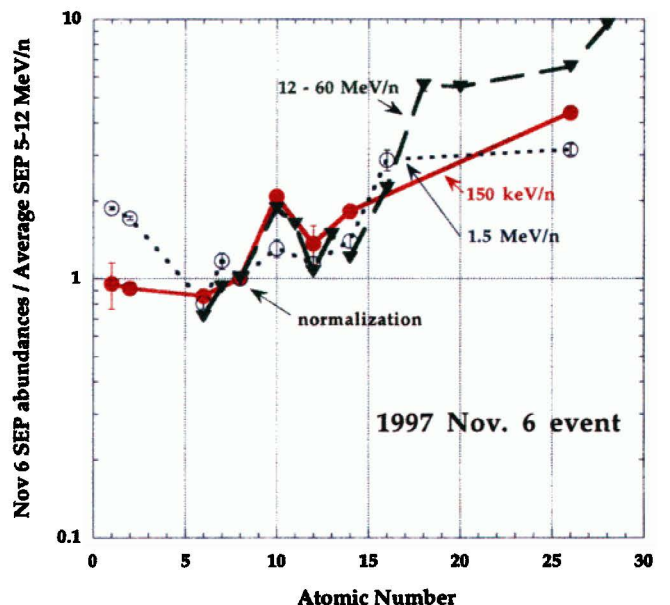


Figure 3. ACE composition during the Nov. 6 event compared to 5-12 MeV/n SEP average abundances.

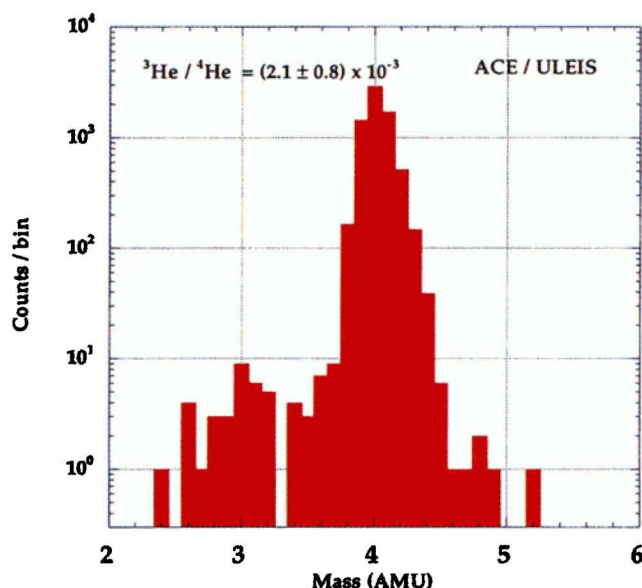


Figure 4. 0.5 - 2.0 MeV/n helium mass histogram measured during day 312.25 through 314.0.

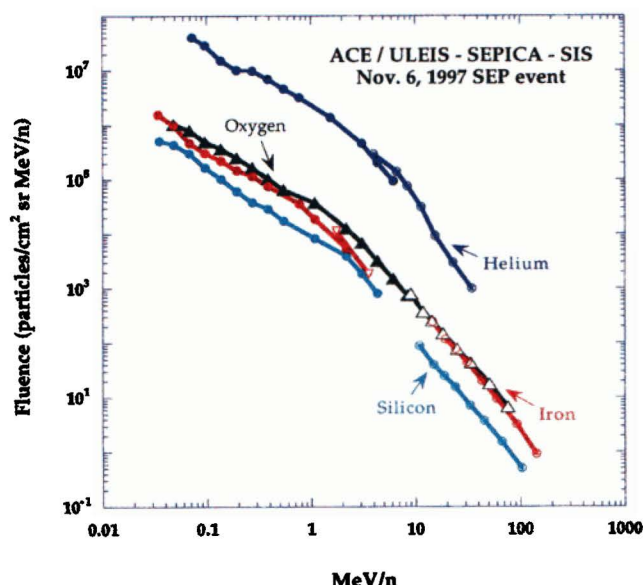


Figure 5. ACE fluences for the Nov. 6 event: He in blue; O in green; Si in light blue; Fe in red. At high energies Fe and O spectra are nearly indistinguishable.

therefore show fluences for several elements in Figure 5. The time intervals used in Figure 5 were chosen at low energies to avoid the shock passage on day 310, while at high energies the entire event interval could be used since the shock did not produce significant numbers of high energy particles. At high energies, the O and Fe fluence spectrum is reasonably well represented by a power law in kinetic energy per nucleon with slope -2.1 [Cohen *et al.*, 1998], while below ~ 1 MeV/n it hardens significantly, with slope -1.1 . The energy at which the spectral break occurs is difficult to identify precisely, but the data can be reasonably described as showing a break at 6-7 MeV/n for Helium, 2-3 MeV/n for O and Si, and ~ 1.5 MeV/n for Fe. Assuming typical SEP ionization states, this corresponds to a rigidity of ~ 200 MV. The Nov. 4 event also showed a roll over of the spectra at similar energies, but it was less pronounced.

Discussion

Following previous work cited above, and based on the radio emission and CMEs observed during this period, we interpret the low energy interplanetary particle population in these events as arising from acceleration at large scale shocks moving outward from the Sun. Although observations at 1 AU cannot uniquely separate the time duration of the particle injection from propagation time, we can roughly estimate upper limits of the duration of the injection by assuming that the major portion of the injection must be complete by the time of maximum intensity at 1 AU. The first 2 rows of Table 1 show such estimates for the Nov. 4 along with an assumed linear propagation rate for the Nov. 4 shock, which arrived at Earth about 64 hours after the optical flare. The third row shows corresponding estimates for the Nov. 6 ground level neutron monitor response, which peaked approximately 2 hours after that flare. While these are

admittedly crude estimates, they indicate that the lowest energy particles could have been accelerated by the shock out to sizable fractions of 1 AU, while for the higher energies the acceleration occurred within roughly 0.1 AU. Lockwood *et al.* [1990] have made comparable injection time estimates using 20 MeV-2 GeV protons, concluding that the injection time scaled as $1/\sqrt{E}$, while at high energies Kahler [1994] used 470 MeV to 4 GeV protons intensity observations to estimate CME injection heights of 5-15 solar radii (R_s).

Simple models of the flare spectra injected at the sun and followed by interplanetary propagation will lead to smoothly varying intensities and abundance ratios at all energies. We interpret the observed low energy deviations from such "smooth" profiles as clues to details of the acceleration and transport. The fluctuations observed, e.g., in the low energy Fe/O ratio in Figure 2 could be due to spatial differences in the seed population sampled as the shock moves through interplanetary space; or, they might arise from changing connections to different portions of the shock. The long term decay seen in the Fe/O ratio at high energies is often observed, and may be a propagation effect arising from the different charge-to-mass ratios of Fe and O.

A major feature is the difference in intensities in the two particle events: compared to the Nov. 4 event, the Nov. 6 event peak intensities are ~ 10 times larger at high energies, and ~ 5 -10 times smaller at low energies. Clearly, the Nov. 6 event at the Sun was much bigger – and this difference is reflected in the peak intensities down to ~ 1 -2 MeV/n. Since the high energy acceleration episode in the Nov. 6 event produced much higher intensities than Nov. 4, we presume that this was the case close to the Sun for low energy particles as well. However, at 1 AU passage, the interplanetary shock for the Nov. 6 event was

Table 1. Estimate of injection duration upper limits and corresponding shock travel

Energy	time to maximum	"direct" propagation time to 1 AU	Upper limit of injection time from flare	Upper limit of shock radial location at end of injection
60 keV/n	50 hr	17 hr	33 hr	0.5 AU 100 R_s
8.9 MeV/n	8.2 hr	1.4 hr	6.8 hr	0.1 AU 23 R_s
relativistic	2 hr	<0.5 hr	~ 1.5 hr	0.025 AU $\sim 5 R_s$

smaller and produced only moderate intensity increases at low energies. The difference in high vs. low energy intensities is presumably due to the fact that at low energies the particles observed at 1 AU are dominated by the interplanetary phase of the acceleration (Table 1), and that while the nose of the shock from the Nov. 4 event passed close to Earth, in contrast the nose of the shock from the Nov. 6 event was significantly westward of Earth when it passed 1 AU. Cane et al. [1988] have shown that the west flank of shocks produce weak particle increases, as observed here for low energies during the second event.

In the case of the Nov. 6 event, different features fall into the often-used classes of "impulsive" and "gradual" events: the high Fe/O ratios and presence of gamma rays are typical of impulsive events; the long duration, slow rises at low energies, and CMEs typical of "gradual" events. Cliver [1996] has proposed mixtures of these classes in which an initial burst of particles with impulsive event characteristics is followed by CME accelerated particles with gradual event characteristics. The Fe/O decrease for the Nov. 6 event seen immediately at high energies, and beginning around day 312.5 at low energies, could be evidence for this, but the subsequent slow decrease of the Fe/O ratio is different from the Cliver model, which would predict "core to halo" transition with an initial high value (~ 1) followed by a distinct change to levels typical of gradual events (~ 0.1). Additionally, the factor of 4 enrichment of ^3He reported here is much lower than the expectation for impulsive events (factors of 1,000-10,000), and also shows no time variation, indicating that the acceleration history of these particles is similar to that of the other heavy ions. A puzzling aspect of the abundances observed here is the simultaneous enhancement of both low mass-to-charge ratio species (^3He) and high mass-to-charge ratio species (Fe) compared to reference elements ^4He and ^{16}O that have mass-to-charge ratio of ~ 2 . This unexpected pattern might be related to other isotopic anomalies observed in this event [Leske et al., 1998].

The spectral hardening that occurs in the \sim few MeV/n range raises many interesting questions. Since shocks produce power law spectra, presumably near the Sun there was originally a single power law spectrum in the energy range well above the injection threshold [Lee, 1983], but by the time the particles reached 1 AU there was a depletion at low energies. This might be due to adiabatic deceleration, which would be more important for low energy particles. However, the opposite behavior, namely a hardening of the spectra at higher energies, has also been observed in the Nov. 22, 1977 SEP event [Beeck et al., 1987]. Clearly, additional observations will be required to understand this issue.

Comparing the low and high energy populations observed in these events, we have seen striking differences in relative composition, absolute intensity, temporal variations, and spectral form. Taken together, these point to multiple seed populations and acceleration regimes operating in these events. The changes in particle ionization state as a function of energy below a few MeV/n reported elsewhere in this issue [Mazur et al., 1998; Möbius et al., 1998b] also strongly suggest a multiple seed populations e.g., coronal vs. nearer the flare site.

Acknowledgements. We thank the many individuals at the University of Maryland, Caltech, Jet Propulsion Laboratory, NASA Goddard Space Flight Center, Johns Hopkins Univ. / APL, and University of New Hampshire for the construction of the instruments. We thank C. Smith and D. McComas and the ACE MAG and SWEPAM teams for the shock identifications used here; R. Lepping and the Wind MFI team for the magnetic cloud identification; K. Ogilvie and the Wind SWE team for the solar wind speeds. This work was supported in part by NASA grants NAG 5-7228, NAG5-6912 and PC 251428.

References

- Beeck, J., G. M. Mason, D. C. Hamilton, et al., A multi-spacecraft study of the injection and transport of solar energetic particles, *Astrophys. J.*, **322**, 1052, 1987.
- Cane, H. V., D. V. Reames, and T. T. von Rosenvinge, The role of interplanetary shocks in the longitude distribution of solar energetic particles, *J. Geophys. Res.*, **93**, 9555, 1988.
- Cliver, E. W., *Solar flare gamma-ray emission and energetic particles in space*, in *High energy solar physics workshop, GSFC*, R. Ramaty, N. Mandzhavidze, and X.-M. Hua, Editor. 1996, AIP press: Woodbury, N.Y. p. 45.
- Cohen, C. M. S., A. C. Cummings, R. A. Leske, et al., Inferred charge states of high energy solar particles from the Solar Isotope Spectrometer on ACE, *Geophys. Res. Letters*, *this issue*, 1998.
- Cook, W. R., E. C. Stone, and R. E. Vogt, Elemental composition of solar energetic particles, *Astrophys. J.*, **279**, 827, 1984.
- Kahler, S., Injection profiles of solar energetic particles as functions of coronal mass ejection heights, *Astrophys. J.*, **428**, 837, 1994.
- Lee, M. A., Coupled hydromagnetic wave excitation and ion acceleration at interplanetary traveling shocks, *J. Geophys. Res.*, **88**, 6109, 1983.
- Leske, R. A., C. M. S. Cohen, A. C. Cummings, et al., Unusual isotopic composition of solar energetic particles observed in the November 6, 1997 event, *Geophys. Res. Letters*, *this issue*, 1998.
- Lockwood, J. A., H. Debrunner, and E. O. Flückiger, Indications for diffusive coronal shock acceleration of protons in selected solar cosmic ray events, *J. Geophys. Res.*, **95**, 4187, 1990.
- Mason, G. M., G. Gloeckler, and D. Hovestadt, Temporal variations of nucleonic abundances in solar flare energetic particle events. II. Evidence for large scale shock acceleration, *Astrophys. J.*, **280**, 902, 1984.
- Mason, G. M., R. E. Gold, S. M. Krimigis, et al., The Ultra Low Energy Isotope Spectrometer (ULEIS) for the ACE spacecraft, *Space Sci. Rev.*, *in press*, 1998.
- Mazur, J. E., G. M. Mason, B. Klecker, et al., The abundances of hydrogen, helium, oxygen, and iron accelerated in large solar particle events, *Astrophys. J.*, **404**, 810, 1993.
- Mazur, J. E., G. M. Mason, M. D. Looper, et al., Charge states of solar energetic particles using the geomagnetic cutoff technique: SAMPEX measurements in the 6 November 1997 solar particle event, *Geophys. Res. Lett.*, *this issue*, 1998.
- Möbius, E., D. Hovestadt, B. Klecker, et al., The Solar Energetic Particle Ionic Charge Analyzer (SEPICA) and the Data Processing Unit (S3DPU) for SWICS, SWIMS, and SEPICA, *Space Sci. Rev.*, *in press*, 1998a.
- Möbius, E., M. Popecki, B. Klecker, et al., Energy dependence of the ionic charge state distribution during the November 1997 solar energetic particle event, *Geophys. Res. Letters*, *this issue*, 1998b.
- Ogilvie, K. W., M. A. Coplan, P. Bochsler, et al., Abundance ratios of $^4\text{He}^{++}/^3\text{He}^{++}$ in the solar wind, *J. Geophys. Res.*, **85**, 6021, 1980.
- Ramaty, R. and R. J. Murphy, Nuclear processes and accelerated particle in solar flares, *Space Sci. Rev.*, **45**, 213, 1987.
- Reames, D. V., Coronal abundances determined from energetic particles, *Adv. Space Res.*, **15**, 41, 1995.
- Reinhard, R. and G. Wibberenz, Propagation of flare protons in the solar atmosphere, *Solar Physics*, **36**, 473, 1974.
- Stone, E. C., C. M. S. Cohen, W. R. Cook, et al., The Solar Isotope Spectrometer for the Advanced Composition Explorer, *Space Sci. Rev.*, *in press*, 1998.
- Van Hollebeke, M. A. I., F. B. McDonald, and J. P. Meyer, Solar energetic particle observations of the 1982 June 3 and 1980 June 21 gamma-ray/neutron events, *Astrophys. J. (Suppl.)*, **73**, 285, 1990.
- von Rosenvinge, T. T., L. M. Barbier, J. Karsch, et al., The energetic particles: acceleration, composition, and transport (EPACT) investigation on the Wind spacecraft, *Space. Sci. Rev.*, **71**, 155, 1995.

(Received September 4, 1998; revised November 2, 1998; accepted November 11, 1998)